Human Molecular Genetics, 2019, Vol. 38, No. 17 2965–2975

doi: 10.1093/hmg/ddz115
Advance Access Publication Date: 20 May 2019
General Article

GENERAL ARTICLE

Learning impairments and molecular changes in the brain caused by β-catenin loss

Robert J. Wickham, Jonathan M. Alexander, Lillian W. Eden, Mabel Valencia-Yang, Josué Llamas, John R. Aubrey and Michele H. Jacob*

Department of Neuroscience, Sackler Biomedical Graduate School, Tufts University School of Medicine, Boston, MA 02111, USA

*To whom correspondence should be addressed at: Department of Neuroscience, Sackler Biomedical Graduate School, Tufts University School of Medicine, 136 Harrison Avenue, Boston, MA 02111, USA. Tel: 617-636-2429; Fax: 617-636-2413; Email: Michele.Jacob@Tufts.edu

Abstract

Intellectual disability (ID), defined as IQ<70, occurs in 2.5% of individuals. Elucidating the underlying molecular mechanisms is essential for developing therapeutic strategies. Several of the identified genes that link to ID in humans are predicted to cause malfunction of β-catenin pathways, including mutations in *CTNNB1* (β-catenin) itself. To identify pathological changes caused by β-catenin loss in the brain, we have generated a new β-catenin conditional knockout mouse (β-cat cKO) with targeted depletion of β-catenin in forebrain neurons during the period of major synaptogenesis, a critical window for brain development and function. Compared with control littermates, β-cat cKO mice display severe cognitive impairments. We tested for changes in two β-catenin pathways essential for normal brain function, cadherin-based synaptic adhesion complexes and canonical Wnt (Wingless-related integration site) signal transduction. Relative to control littermates, β-cat cKOs exhibit reduced levels of key synaptic adhesion and scaffold binding partners of β-catenin, including N-cadherin, α-N-catenin, p120ctn and S-SCAM/Magi2. Unexpectedly, the expression levels of several canonical Wnt target genes were not altered in β-cat cKOs. This lack of change led us to find that β-catenin loss leads to upregulation of γ-catenin (plakoglobin), a partial functional homolog, whose neural-specific role is poorly defined. We show that γ-catenin interacts with several β-catenin binding partners in neurons but is not able to fully substitute for β-catenin loss, likely due to differences in the N-and C-termini between the catenins. Our findings identify severe learning impairments, upregulation of γ-catenin and reductions in synaptic adhesion and scaffold proteins as major consequences of β-catenin loss.

Introduction

Intellectual disability (ID; IQ<70) is a prevalent developmental brain disorder that occurs in 2.5% of the general population (1–5). Effective pharmacotherapeutic interventions are lacking because the molecular etiology is poorly defined. Emerging evidence from human genetic studies suggests that gene mutations that cause loss of function of β-catenin pathways link to ID (6–11). Individuals with disruptive mutations in *ctnnb1*, which encodes β-catenin, exhibit high penetrance for ID (7–9). They typically also display microcephaly, motor and speech delays, reduced muscle tone and increased anxiety. The tight correlation between β-catenin malfunction and ID presents a valuable opportunity to gain critical insights into the underlying molecular changes in the brain *in vivo*.

β-catenin plays key roles in two pathways that are essential for normal brain development and function, cadherin-based synaptic adhesion complexes and canonical Wnt signal transduction. β-catenin is recruited to synapses by binding to the intracellular domain of N-cadherin; it links the synaptic

Received: March 7, 2019. **Revised:** May 20, 2019. **Accepted:** May 22, 2019

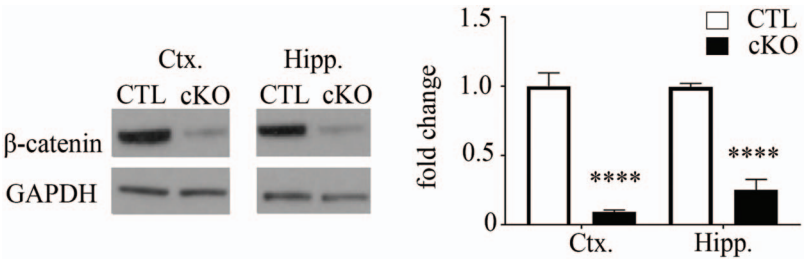

Figure 1. β-catenin conditional knockout in mouse forebrain neurons. (Left) Western blot showing β-catenin protein levels are dramatically decreased in cortical (ctx) and hippocampal (hipp) lysates of β-cat cKO mice at 3 months of age. β-catenin deletion is driven by CAMKII promoter-dependent expression of Cre recombinase in forebrain postmitotic excitatory neurons. (Right) Histogram of decreased β-catenin levels in the indicated brain region lysates of β-cat cKO mice, relative to control littermate levels. Signals are normalized to GAPDH as a loading control (****$P < 0.0001$, Student's *t*-test, $n = 9$ β-cat cKO mice and $n = 9$ control littermates).

adhesion complex to the submembranous actin cytoskeleton, via binding to α-N-catenin, thereby stabilizing the synapse (12–15). Additionally, β-catenin binds directly to key postsynaptic scaffolds, the synaptic scaffolding cell adhesion molecule (S-SCAM/Magi2) and adenomatous polyposis coli protein that bring together other adhesion proteins, glutamate receptors and signaling molecules that impact synapse maturation and function (16–19). In the canonical Wnt signaling pathway, β-catenin functions as a transcription co-activator with TCF/LEF. Synaptic activity induces the release of soluble Wnt, which binds to its cognate receptors on the neuron surface, activates downstream signals, leading to β-catenin stabilization and translocation to the nucleus where it mediates Wnt responsive gene expression (20–22). Abnormal Wnt signaling and abnormal synaptic adhesion in the developing brain alter axon guidance cues, synapse differentiation, plasticity and network connectivity (13,14,23–30).

Our study provides new insights into how *Ctnnb1* disruptive mutations (β-catenin loss-of-function) affect these two key pathways in the brain and lead to ID. We have generated a new conditional knockout mouse targeting β-catenin deletion predominantly in excitatory neurons of the forebrain during the early postnatal stage of major synaptic differentiation, a critical period of brain development (31). This timing differs from other published studies of β-catenin loss of function (31–33).

We show here that our β-catenin conditional knockout mouse (β-cat cKO) line displays severely impaired learning, as seen in individuals with loss-of-function mutations in *Ctnnb1*. Unexpectedly, we find that β-catenin depletion leads to increased levels of γ-catenin, a partial functional homologue that is normally expressed at low levels in brain neurons (34). We show that γ-catenin can substitute for only some of β-catenin's neural functions. Our findings provide critical insights into molecular changes associated with severe cognitive deficits and identify new targets with potential for ameliorating the impairments caused by β-catenin loss.

Results

New β-cat cKO line

To gain insights into the molecular etiology of ID caused by loss-of-function mutations in *Ctnnb1*, we have generated a new mouse model of β-catenin loss in neurons. We targeted β-catenin depletion during the period of major synaptogenesis, a critical stage of brain development. We crossed *ctnnb1*$^{fl/fl}$ lox468/lox468 mice (35) with mice expressing Cre-recombinase under control of the CamKIIα promoter (18,36). Previous reporter gene expression studies show that this Cre93 mouse line drives Cre recombinase expression during synaptogenesis, beginning at late embryonic ages, with full activation by postnatal day (P) 21, in cortical and hippocampal excitatory glutamatergic neurons (18,31,36). We have confirmed β-catenin protein depletion in the β-cat cKO mouse brain by showing dramatic reductions in the hippocampus and cortex, relative to wild-type littermates, using quantitative immunoblotting (Fig. 1, Ctx: Control 1.00 ± 0.09; cKO 0.09 ± 0.01; $t_{16} = 9.31$; Student's *t*-test $P < 0.0001$; Hipp: Control 1.00 ± 0.03; cKO 0.25 ± 0.07; $t_{18} = 10.21$; $P < 0.0001$). Small amounts of β-catenin protein remaining likely derive from glial cells and interneurons, as β-catenin is ubiquitously expressed, but α-CaMKII-Cre transgene is not expressed in these cell types (18,36).

β-catenin loss of function leads to severe cognitive impairments

Because individuals with *Ctnnb1* disruptive gene mutations exhibit ID, we tested for altered cognitive function in β-cat cKO mice, relative to control littermates. We assessed the β-cat cKOs for hippocampal-dependent learning impairments using two separate behavioral tasks for evaluating learning and memory. In the contextual fear-conditioning task, β-cat cKO mice exhibited severe learning deficits [Fig. 2A, genotype $F_{1,27} = 15.18$, $P < 0.0001$; time $F_{6,162} = 25.39$, $P < 0.0001$; genotype X time $F_{6,162} = 5.069$, $P < 0.0001$; two-way Analysis of variance (ANOVA)-repeated measures (RM)]. They showed little improvement in their performance, never reaching the freezing level of control littermates over the course of training (7 days). Because of the lack of learning, they were not able to be tested for memory deficits in probe trial tests. Pain threshold, as measured by a latency to paw lick on a heated plate, was not different between genotypes (Control 14.81 ± 1.12; cKO 14.09 ± 1.51; $t_{27} = 0.38$, $P = 0.71$, Supplementary Material, Fig. S1A), suggesting that the poor performance of the β-cat cKOs is due to cognitive deficits, but not sensory defects such as reduced sensitivity to the foot shock.

We next tested for spatial learning and memory deficits using the Barnes Maze. β-cat cKOs were unable to learn the location of the goal hole over the course of training (up to eight trials) (Fig. 2B, main effect of genotype $F_{1,37} = 17.78$, $P < 0.0001$; main effect of time $F_{7,259} = 22.04$, $P < 0.0001$; interaction of genotype and time $F_{7,259} = 4.663$, $P < 0.0001$; two-way ANOVA) and could not proceed to probe trials. We found no changes between genotypes in movement speed during the task (Control 4.83 ± 0.40; cKO 4.63 ± 0.49; $t_{32} = 0.30$, $P = 0.77$, Student's *t*-test, Supplementary Material, Fig. S1B), removing the confound of locomotion or exploratory behavior changes due to motor defects. These data suggest that the lack of β-catenin during

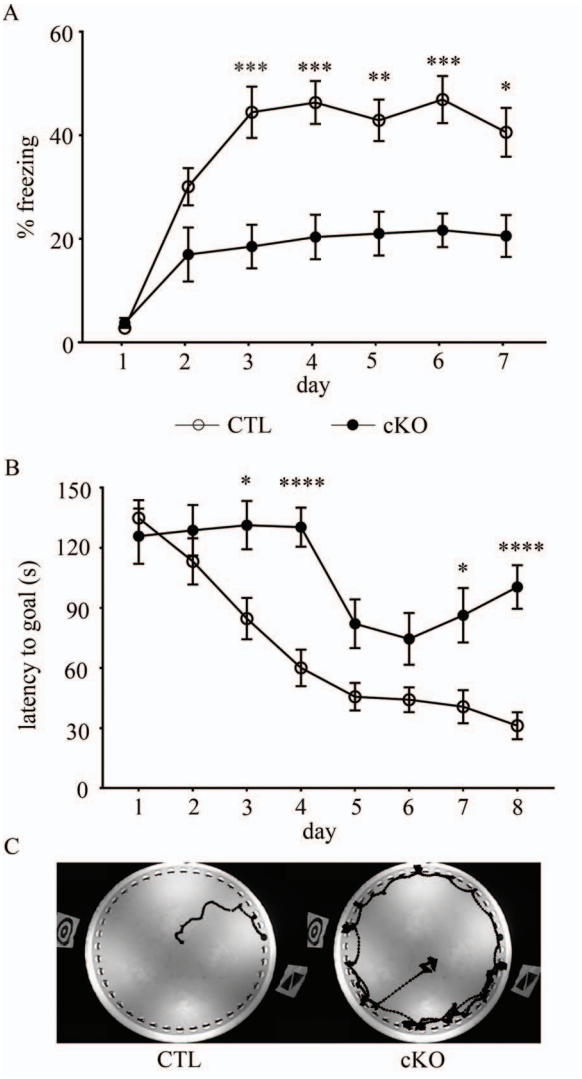

Figure 2. β-cat cKOs display severe learning impairments. In two different cognitive tasks, β-cat cKOs showed severe learning deficits based on little improvement in their performance over the training period, as seen in **(A)** their percent freezing in the contextual fear conditioning assay and **(B and C)** their latency to learn the location of the goal hole, using wall-mounted spatial cues, in the Barnes maze task. In sharp contrast, control littermates showed rapid improvement and learned both tasks (*$P < 0.05$; **$P < 0.01$; ***$P < 0.001$; ****$P < 0.0001$, two-way ANOVA with Bonferonni corrected *t*-test, $n = 10$ β-cat cKO mice and $n = 19$ control littermates).

synaptic differentiation in forebrain excitatory neurons causes severe cognitive impairments.

β-cat cKOs do not display ASD-like behaviors

In addition to ID as the major phenotype, loss-of-function mutations in human *Ctnnb1* may also lead to autism (37). Thus, we tested β-cat cKOs using diagnostic assays designed to test for relevant autism-like behaviors (altered social interest and repetitive behaviors) in mice (38). In the classic three-chambered social interaction task, β-cat cKOs and their littermate controls both displayed a similar preference for interacting with the caged novel mouse versus a caged nonsocial object (Fig. 3A, genotype $F_{1,20} = 0.01$, $P = 0.17$; object $F_{1,20} = 61.98$, $P < 0.0001$; genotype X time $F_{1,20} = 0.0001$, $P = 0.99$; two-way ANOVA-RM; Control social stimulus 109.8 ± 14.51, nonsocial stimulus 19.41 ± 3.10; cKO social stimulus 108.4 ± 14.53, nonsocial stimulus 18.32 ± 4.30).

We then tested for altered repetitive behaviors using the marble burying assay. Increased marble burying reflects repetitive digging behavior and does not correlate with anxiety-related measures (18,39). β-cat cKOs and littermate controls buried a similar amount of marbles (Fig. 3B, Control 2.4 ± 0.31; cKO 2.9 ± 0.56; $t_{53} = 0.84$, $P = 0.41$, Student's *t*-test). These data suggest that loss of β-catenin in excitatory forebrain neurons does not cause autism-like behaviors.

β-cat cKOs exhibit increased anxiety

Because a subset of individuals with *Ctnnb1* disruptive mutations also display increased anxiety or motor deficits, we tested for these phenotypes in our β-cat cKO mouse model. Further, mouse studies of *Ctnnb1* in the nucleus accumbens show a critical role in regulating anxiety through micro-RNA-dependent mechanism (40). Our β-cat cKOs exhibited increased anxiety-like behavior in the open field test, spending significantly less time exploring the open portion of the arena compared to littermate controls (Fig. 3C, Control 10.27% ±1.70%; cKO 2.47% ±0.94%; $t_{57} = 3.742$, $P < 0.001$, Student's *t*-test). They displayed no differences in total exploration distance, suggesting no motor impairments (Fig. 3D, Control 3773 ± 245, cKO 3374 ± 376, $t_{57} = 0.939$, $P = 0.38$). As a separate test of anxiety, we used the light/dark box assay. β-cat cKOs spent significantly less time in the lit box compared to littermate controls (Fig. 3E, Control 26.89% ± 3.36%; cKO 9.99% ±2.33%; $t_{19} = 3.86$, $P < 0.01$, Student's *t*-test). To further assess motor function as a potential confound, we used 24 h home cage monitoring. Overall locomotor behavior was comparable between β-cat cKOs and littermate controls (Fig. 3F, Control $51\,801 \pm 6485$; cKO $43\,161 \pm 11\,846$; $t_{12} = 0.64$, $P = 0.53$, Student's *t*-test). In the rotorod test, which assesses motor coordination, we observed no differences in performance between the genotypes (Fig. 3G, Control 25.15 ± 0.99; cKO 26.25 ± 1.24; $t_{20} = 0.70$, $P = 0.49$, Student's *t*-test). Again, we found no difference in movement speed in the Barnes Maze task. Thus, β-cat cKOs show normal locomotion and motor function. However, they exhibit increased anxiety.

Normal Wnt target gene expression levels

To begin to define molecular changes in the brain caused by β-catenin loss, we focused on its dual roles in the canonical Wnt signal transduction pathway and cadherin-containing synaptic adhesion complexes, pathways required for normal synaptic function, stability and plasticity. Given that β-catenin is the major mediator of canonical Wnt-stimulated gene transcription (41), we anticipated finding reduced expression levels in the β-cat cKO brain. Unexpectedly, the mRNA levels of several Wnt targets previously found to be responsive to changes in β-catenin levels or function (18,42–44) were normal in the β-cat cKO cortex (Fig. 4A), relative to control littermates, including *c-myc* (Control 1.00 ± 0.06, cKO 0.99 ± 0.10, $t_{13} = 0.01$, $P = 0.99$, unpaired *t*-test), *dkk1* (Control 1.00 ± 0.18, cKO 1.425 ± 0.224, $t_{13} = 1.49$, $P = 0.16$), *cycd1* (Control 1.00 ± 0.04, cKO 0.67 ± 0.11, $t_{12} = 1.49$, $P = 0.19$), *c-met* (Control 1.00 ± 0.18, cKO 1.31 ± 0.24, $t_{12} = 1.03$, $P = 0.32$), *lef1* (Control 1.00 ± 0.05, cKO 1.20 ± 0.16, $t_{12} = 1.44$, $P = 0.17$) and *syn2* (Control 1.00 ± 0.02, cKO 1.02 ± 0.07, $t_{14} = 0.27$, $P = 0.79$). We found similar results in the β-cat cKO hippocampus (Supplementary Material, Fig. S2A) for *c-myc* (Control 1.00 ± 0.04,

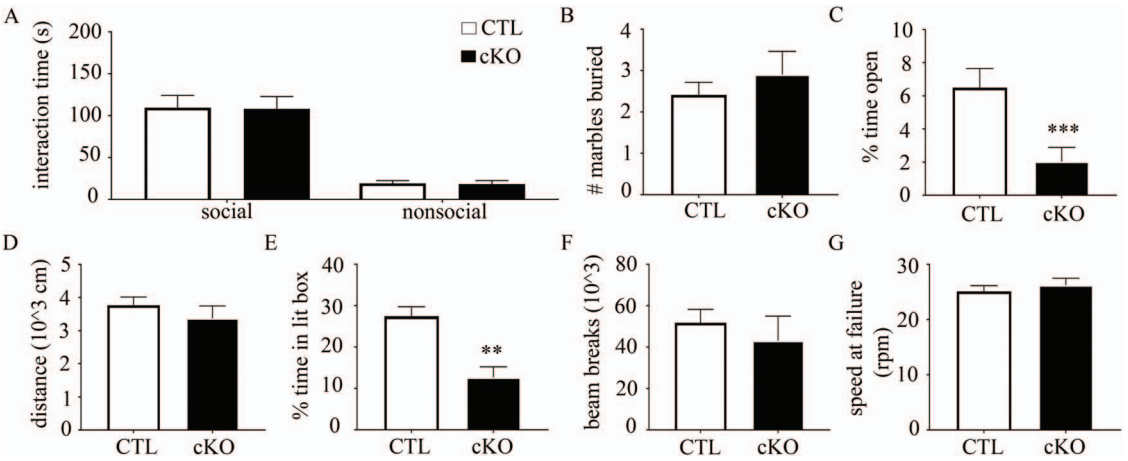

Figure 3. β-cat cKOs exhibit increased anxiety, but no autism-like behaviors or motor impairments. **(A)** In the three-chambered social interaction assay, β-cat cKOs and wild-type littermates showed a similar preference for interacting with a caged, novel mouse over a caged, novel object. **(B)** β-cat cKOs and wild-type littermates buried a similar number of marbles in the marble burying task, suggesting no aberrant repetitive behaviors. **(C)** Compared to littermate controls, β-cat cKOs exhibit increased anxiety, as they spend less time in the center during the open field test. **(D)** β-cat cKOs have normal locomotion, based on the distance traveled in the open field test. **(E)** In the light/dark box assay, β-cat cKOs spend less time in the lit portion of the chamber, further suggesting increased anxiety. **(F)** Monitoring home cage behavior shows similar levels of motor activity between β-cat cKOs and littermate controls. **(G)** β-cat cKOs display normal motor coordination in the rotorod test.

cKO 0.87 ± 0.08, $t_{13} = 1.38$, $P = 0.19$), *dkk1* (Control 1.00 ± 0.20, cKO 1.19 ± 0.38, $t_{12} = 0.44$, $P = 0.66$) and *syn2* (Control 1.00 ± 0.20, cKO 0.96 ± 0.162, $t_{13} = 0.12$, $P = 0.91$).

Upregulation of γ-catenin, a partial function homologue of β-catenin

The normal levels of Wnt target gene expression in the absence of β-catenin suggested possible functional compensation. γ-catenin is a partial functional homologue of β-catenin. Normally, it is expressed at low levels, relative to β-catenin, in neurons (34) and its neural function is poorly defined. Studies in non-neuronal cells show that γ-catenin is primarily enriched in desmosomal junctions and to a lesser extent, adhesion junctions (22,45). Thus, we first tested whether γ-catenin levels are altered in the β-cat cKO brain. Indeed, γ-catenin levels showed 4-fold increases in the β-cat cKO hippocampus (Fig. 4B, Control 1.00 ± 0.14, cKO 3.6 ± 0.30, $t_{18} = 8.11$, $P < 0.001$) and cortex (data not shown; Ctl 1.00 ± 0.15, cKO 3.5 ± 0.30; $t_{16} = 7.67$, $P < 0.001$) compared with littermate controls.

Next we tested for γ-catenin interactions with LEF-1, the main transcriptional co-activator of canonical Wnt target gene expression. Nuclear LEF-1 levels were normal in the β-cat cKO hippocampus (Fig. 4D, 1.00 ± 0.14, cKO 0.95 ± 0.20, $t_6 = 0.222$, $P = 0.83$, Student's *t*-test). However, we found increased association of γ-catenin with LEF-1 by co-immunoprecipitation with hippocampal lysates from β-cat cKOs, compared to littermate controls (Fig. 4B, IP, cKO 1.45 ± 0.06, $t_2 = 8.23$, $P < 0.05$, one-sample *t*-test). These findings suggest that Wnt target gene expression is likely maintained by compensatory increases in γ-catenin, in the absence of β-catenin.

Reduced levels of β-catenin synaptic partners

Next we tested for changes in the N-cadherin-based synaptic adhesion complex, focusing on β-catenin direct binding partners. We found reductions in the N-cadherin transmembrane adhesion protein in frontal cortical lysates of β-cat cKOs, compared to littermate controls (Fig. 5A, Control 1.00 ± 0.04, cKO 0.75 ± 0.03; $t_{16} = 4.61$, $P < 0.001$, unpaired *t*-test). Similarly, we found reduced levels of α-n-catenin, which stabilizes the synapse by linking N-cadherin to the actin cytoskeleton via β-catenin (Fig. 5A, Control 1.00 ± 0.05, cKO 0.43 ± 0.06; $t_{14} = 10.45$, $P < 0.0001$, unpaired *t*-test). Further, β-cat cKOs also exhibit decreases in p120 catenin (Fig. 5A, Control 1.00 ± 0.14, cKO 0.34 ± 0.08, $t_{16} = 3.89$, $P < 0.01$). p120 catenin binds to N-cadherin and coordinates signaling between cadherins and Rho-family GTPases to regulate cytoskeletal changes that impact synapse formation, spine density and dendritic arborization (46–49). Additionally, similar reductions in these β-catenin binding partners were seen in the hippocampus (N-cadherin, Control 1.00 ± 0.02, cKO 0.69 ± 0.10, $t_9 = 3.19$, $P < 0.05$; α-N-catenin, Control 1.00 ± 0.08, cKO 0.27 ± 0.03; $t_9 = 7.81$, $P < 0.001$; p120 catenin, Control 1.00 ± 0.03, cKO 0.52 ± 0.08, $t_{14} = 5.36$, $P < 0.001$; Supplementary Material, Fig. S2B). These findings suggest that γ-catenin cannot fully substitute for the loss of β-catenin at the synaptic complex. We therefore tested for γ-catenin association with these β-catenin binding partners in the β-cat cKO mouse brain.

Despite reductions in their total levels, both N-cadherin and α-N-catenin displayed increased levels of co-immunoprecipitation with γ-catenin in β-cat cKOs, compared to littermate controls (Fig. 5B N-cadherin, IP, cKO 5.31 ± 0.80, $t_{(3)} = 5.36$, $P < 0.05$; α-N-catenin, IP, cKO 15.43 ± 1.90, $t_{(4)} = 7.69$, $P < 0.01$, one-sample *t*-test). The ratio of N-cadherin co-immunoprecipitated by γ-catenin to total N-cadherin levels was 8-fold higher (Fig. 5B, N-cadherin, IP/input, cKO 7.89 ± 2.10, $t_{(3)} = 3.331$, $P < 0.05$, one-sample *t*-test) and the ratio of α-N-catenin co-immunoprecipitated by γ-catenin to total α-N-catenin levels was 35-fold higher (Fig. 5B, α-N-catenin, IP/input, cKO 35.27 ± 4.52, $t_{(4)} = 7.56$, $P < 0.01$, one-sample *t*-test). However, our data suggest that γ-catenin cannot stabilize these synaptic binding partners.

We then tested for altered levels of the postsynaptic scaffolding protein S-SCAM/MAGI-2. S-SCAM binds to β-catenin via its C-terminus PDZ (Postsynaptic density protein 95, PSD-95; Discs large, Dlg; Zonula occludens-1 protein, ZO-1) domain, which is lacking in γ-catenin (45). S-SCAM is a key organizer of the postsynaptic multi-protein complex; it binds to and brings

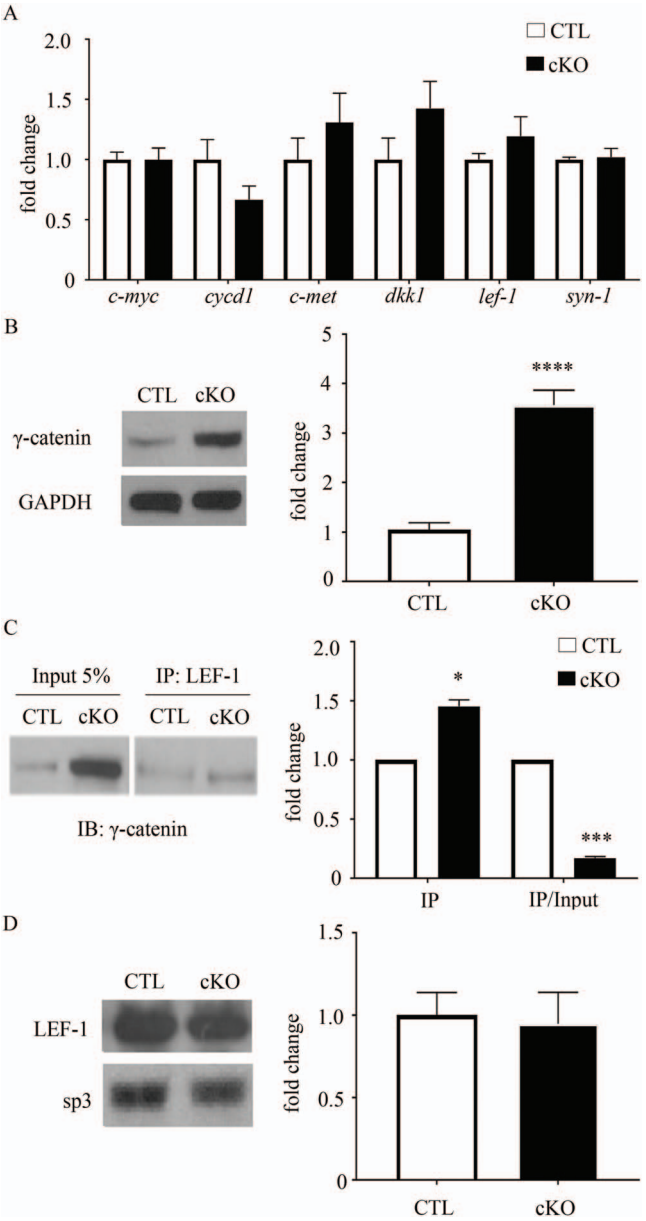

Figure 4. Normal levels of canonical Wnt target gene expression and increased levels of γ-catenin in β-cat cKO forebrain. (A) mRNA levels of several Wnt targets are unchanged in the β-cat cKO frontal cortex, compared to wild-type littermates. **(B)** Representative immunoblot and quantification showing increased levels of γ-catenin in β-cat cKOs. $N = 7$–9 β-cat cKO mice and 7–9 control littermates. **(C)** Co-immunoprecipitation and quantification showing increased association of γ-catenin with LEF-1 in β-cat cKOs. IP = quantification of protein not normalized to input; IP/input = quantification of protein normalized to input. $N = 3$ β-cat cKO mice and 3 control littermates. **(D)** Representative immunoblot demonstrating similar levels of LEF-1 in the nuclear fraction of β-cat cKOs and littermate controls. SP3 transcription factor, as a loading control. $N = 4$ β-cat cKO mice and 4 control littermates. (*$P < 0.05$; **$P < 0.01$; ***$P < 0.001$; ****$P < 0.0001$, Student's *t*-test for (B) and (C), one-sample *t*-test for D).

together synaptic adhesion proteins (neuroligin, sidekick), signaling molecules (phosphatase and tensin homolog), dendrite arborization and synapse maturation 1, NMDA receptors, hyperpolarization-activated cation channels, axin and both β- and α-catenin (16,50). Our β-cat cKO mice exhibit reductions in S-SCAM levels, as measured in hippocampal isolated membrane preparations (Fig. 5C, Control 1 ± 0.11; cKO 0.56 ± 0.08; $t_{(6)} = 3.21$, $P < 0.05$). Our findings suggest that γ-catenin can functionally substitute for β-catenin in canonical Wnt target gene expression, but not in orchestrating the stable retention of synaptic adhesion and scaffold proteins.

Altered synaptic spine density in the absence of β-catenin

β-catenin is known to regulate spine density and stability in cultured neurons via its role in linking N-cadherin to the actin cytoskeleton (51). Further, our β-cat cKO displays decreases in N-cadherin, α-N-catenin and p120ctn synaptic adhesion and cytoskeletal regulators required *in vivo* for spine stability and structural plasticity, particularly at the early stages of synapse formation (30,46,52,53). We therefore tested whether spine density was altered in the β-cat cKO brain. We found modest, but

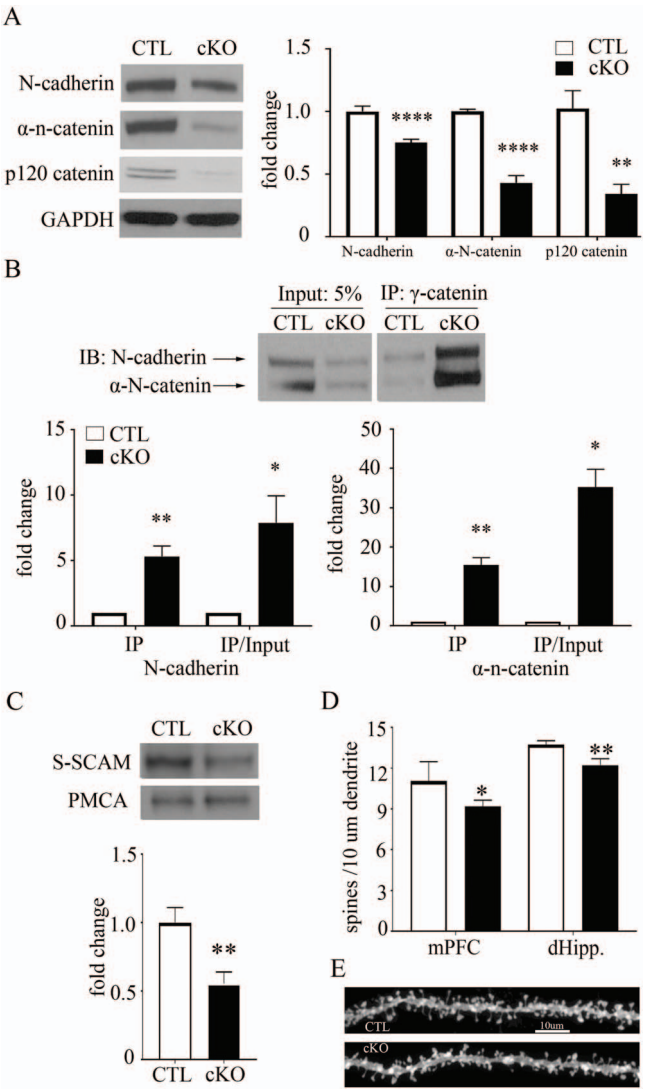

Figure 5. Decreased levels of synaptic adhesion and scaffold proteins and reduced spine density in the β-cat cKO forebrain. **(A)** Representative immunoblot and quantification showing reduced levels of N-cadherin, α-N-catenin and p120 catenin in the β-cat cKO cortex, compared with control littermates. GAPDH, as a loading control. $N = 7–9$ β-cat cKO mice and 7–9 control littermates. **(B)** Co-immunoprecipitation and quantification showing increased association of N-cadherin and α-N-catenin with γ-catenin in the β-cat cKO. IP = quantification of protein not normalized to input; IP/input = quantification of protein normalized to input. $N = 4–5$ β-cat cKO mice and 4 control littermates. **(C)** Immunoblot and quantification showing reduced levels of S-SCAM in membrane fractions prepared from the β-cat cKO and control littermate cortex. PMCA, as a loading control. $N = 4$ β-cat cKO mice and 4 control littermates. **(D)** Histogram showing reduced spine density in layer III of mPFC and CA1 pyramidal neurons (dHipp). $N = 4$ β-cat cKO mice and 4 control littermates, 7–8 neurons per mouse ($^*P < 0.05$; $^{**}P < 0.01$; $^{***}P < 0.001$; $^{****}P < 0.0001$). **(E)** Representative images from control and β-cat cKO CA1 pyramidal neurons. Student's *t*-test for (A), (C) and (D); one-sample *t*-test for (B).

significant, reductions in spine density in pyramidal neuron apical dendrites in both medial prefrontal cortex (mPFC) layer III and dorsal hippocampal (dHipp) CA1 (Fig. 5D and E; mPFC: Ctl 11.05 ± 0.35; cKO 9.18 ± 0.24, $P < 0.05$; dHipp: Ctl 13.72 ± 0.15; cKO 12.21 ± 0.24, $P < 0.01$, Student's *t*-test, $n = 4$ mice per group, 7–8 neurons per mouse). The reductions in spine density and in synaptic binding partners of β-catenin are consistent with the cognitive impairments displayed by β-cat cKOs.

Discussion

Several human gene mutations that link to ID, including *ctnnb1*, are predicted to cause β-catenin malfunction (7–11, 33,54,55). Our findings provide critical mechanistic insights by identifying novel molecular changes caused by β-catenin loss in the brain, *in vivo*. We have developed a new β-cat cKO mouse model that exhibits severe ID. We assessed molecular changes in two key β-catenin pathways essential for normal brain function. Compared with control littermates, β-cat cKOs display reductions in cadherin synaptic adhesion complex and postsynaptic scaffold components that interact with β-catenin. In sharp contrast, canonical Wnt target gene expression levels are not altered, despite the loss of the major mediator of gene transcription in this pathway. This unexpected result led us to discover that β-catenin depletion leads to increases in its partial function homolog, γ-catenin/plakoglobin. The role of γ-catenin in neurons is poorly defined. We show here in the β-cat cKO brain that γ-catenin can substitute for β-catenin in binding to LEF-1 and in mediating normal transcription levels of several Wnt responsive genes. However, γ-catenin cannot

compensate for β-catenin loss at the synapse; we find reduced levels of the β-catenin direct and indirect binding partners N-cadherin, α-N-catenin, p120 catenin and S-SCAM/Magi2. These molecular players are essential for proper synaptic spine density, maturation and plasticity, consistent with the decreases in spine density in β-cat cKO cortical and hippocampal pyramidal neurons. Our findings show that β-catenin's role at cadherin synaptic adhesion and scaffold complexes is essential for normal cognition. We identify synaptic changes, but not Wnt signaling changes, as key to the learning impairments seen with β-catenin loss.

Accumulating evidence supports our findings. The *ctnnb1* 'batface' point mutation (Thr653Lys) causes cognitive impairments in both humans and mice (33). This mutation prevents β-catenin interactions with N-cadherin, leading to loss of its function in the synaptic adhesion complex, while increasing its translocation to the nucleus and β-catenin-mediated Wnt target gene expression (33,56). Whether only one or both of these β-catenin malfunctions cause the learning deficits is undefined. Our findings suggest that reductions in synaptic adhesion are the underlying mechanism that leads to ID. As further support, N-cadherin cKO in mature hippocampal excitatory neurons leads to decreased β-catenin levels, spatial learning deficits (more errors) and impaired long-term spatial memory (57). Deletion of Catna2 (α-N-catenin), which links N-cadherin to the actin cytoskeleton via β-catenin, also causes impaired cognition (58). Similarly, β-catenin deletion in the amygdala prevents normal consolidation of fear memory (59).

Interestingly, β-catenin depletion in distinct brain cell types shows different phenotypes. Our β-cat cKO predominantly targets forebrain excitatory neurons and displays severe ID and increased anxiety-like behavior. A similar β-cat cKO that targets the same cell type at later ages (P21), when there is less synaptogenesis, exhibits depression-like behavior, but cognitive function was not assessed (32). Mice with β-catenin depletion targeted to parvalbumin inhibitory interneurons display autism-like behaviors (reduced social novelty and increased repetitive behaviors), increased anxiety and enhanced spatial memory, but normal contextual fear learning (60). These data suggest neuron subtype-specific mechanisms by which β-catenin malfunction can lead to cognitive and autistic-like behavioral changes. Alternatively, these data may collectively suggest that dysfunction in parvalbumin generally, through reductions in β-catenin as a specific case, may underlie the pathophysiology of autism.

The γ-catenin, a partial functional homolog of β-catenin, is normally expressed at low levels in neurons, relative to β-catenin, and its neural-specific role is poorly defined. It has mostly been studied in non-neuronal cells or olfactory neurons where it functions in focal adhesion complexes (61). We show here that β-catenin loss in neurons leads to upregulation of γ-catenin, but the ability of γ-catenin to compensate for β-catenin's neural functions is limited. Structural differences between the two catenins may explain why. The two catenins share high sequence homology in their central armadillo repeat regions, but little homology in their N- and C-termini (45). The armadillo repeat region of both catenins bind cadherins and LEF-1/TCF. In non-neuronal cells, there is mixed evidence for γ-catenin's ability to completely substitute for β-catenin in driving Wnt target gene expression (22,62), likely due to γ-catenin's lower affinity for LEF-1, compared to β-catenin, possibly due to their terminal tails (22,62–64). This difference likely underlies our findings in the β-cat cKO brain of dramatic increases in γ-catenin levels, but only moderate increases in its association (co-immunoprecipitation) with LEF-1 and normal levels of Wnt target gene expression. Moreover, our data suggest that substitution of γ-catenin for β-catenin is a physiologically and disease-relevant mechanism. Further, β-catenin and γ-catenin both bind to the same site on N-cadherin's C-terminus, but the functional consequences may differ. The β-catenin binding to this site causes PEST sequences in the unstructured C-terminus tail to become inaccessible to ubiquitin and proteasome degradation (65,66). Without β-catenin, cadherins have been shown to be more susceptible to ubiquitination and proteolysis (65). Thus, although γ-catenin binds to this same region of N-cadherin, it may not be able to adequately mask the PEST sequences, leading to greater degradation. Direct tests are needed to confirm this. Consistent with this possibility, we show increased association of γ-catenin with N-cadherin, but reduced N-cadherin levels, in the β-cat cKO brain, compared with control littermates. Further, β-catenin and γ-catenin interact with different isoforms of afadin, that, in turn, have distinct roles in bringing together and stabilizing cadherin complex components at the synapse (67). β-catenin interacts with the long form of afadin (afadin-l), an actin binding scaffolding protein, known to stabilize N-cadherin-based synaptic adhesion complexes and dynamically regulate spine structural plasticity through its interactions with β-catenin, N-cadherin, α-N-catenin, p120ctn and kalirin-7 (67–70). In comparison, γ-catenin has high affinity for the short form of afadin (afadin-s), which lacks the actin binding domain, does not form complexes with β-catenin and α-N-catenin and cannot stabilize adherens junctions (67). This difference may play a role in the decreases in N-cadherin, α-N-catenin and p120ctn displayed by β-cat cKOs. Similarly, both afadin and p120ctn KOs exhibit reductions in N-cadherin and α-N-catenin levels and spine density (70).

As a further difference between β-catenin and γ-catenin, the C-terminus of β-catenin contains a PDZ-binding domain that is required for binding to the postsynaptic scaffolding protein S-SCAM/Magi2 (16). In contrast, γ-catenin lacks the PDZ-binding domain and is therefore incapable of substituting for this β-catenin neural function. We show that S-SCAM levels are reduced in the β-cat cKO brain. Given that β-catenin interacts with additional binding partners via its PDZ-binding domain, including Lin7 (71) and Shank3 (72,73), other synapse organizing roles of β-catenin may also be altered. Future studies are needed to further define the synaptic changes caused by β-catenin loss and the organization of synaptic complexes orchestrated by γ-catenin in the absence of β-catenin.

We provide new insights into the molecular mechanisms by which *ctnnb1* loss-of-function mutations cause ID. We show that β-catenin depletion leads to increases in γ-catenin and that these two catenins have both shared and unique functions in neurons. Synaptic adhesion and scaffold components are selectively altered, whereas Wnt signal transduction is not. We thereby identify new molecular targets to advance the future design of therapeutic strategies to ameliorate ID caused by β-catenin malfunction.

Materials and Methods

Animals

β-cat cKO mice were generated by crossing B6.129-Ctnnb1^{tm2Kem}/KnwJ (β-catenin flox/flox) with CamKIIα-Cre mice (36,37). Cre negative littermates were used as controls for all experiments. Equal numbers of male and female mice were used between the ages of 8 and 16 weeks of age. The mice were housed on a reverse

12 h light/dark cycle and handled 5 min daily for a week before behavioral testing. Diagnostic behavioral assays were performed in the Tufts Center for Neuroscience Research Animal Behavior Facility. All procedures were approved by the Tufts University Institutional Animal Care and Use Committee in accordance with National Institutes of Health guidelines.

Contextual fear conditioning

Fear conditioning trials were performed in a specialized chamber [Coulbourn Instruments, Whitehall, PA; H10-11RTC, 120 cm (W) × 100 (H) × 120 cm (L)] and consisted of 450 s with 2 s, 0.8 mA foot shocks administered at 240, 300, 360 and 420 s. Mice received one trial per day for 7 days. Freezing behavior was measured using a digital camera connected to a computer with Actimetrics FreezeFrame (Wilmette, IL) software. Freezing was scored between 60 s and 240 s of the trial (120 s in total) on each day.

Barnes maze

The Barnes maze was performed as done previously in our laboratory (18). Mice were tested 8 days, two trials per day. On each day, they were given two 3 min trials, spaced 20 min apart. If mice failed to find the goal after 3 min, they were gently guided to the goal and into the escape box. The latency to reach the goal box was averaged for each day.

Three-chamber social interaction test

Three-chamber social interaction test was performed as done previously (18) [adapted from (74)]. Mice were given a 10 min habituation period, followed by a 10 min trial to explore all three chambers, with one side chamber containing a novel, juvenile male mouse (postnatal day 25) within an inverted, cylindrical wire mesh cage, while the other side chamber contained an identical empty, inverted wire mesh cage. Trials were recorded by a video camera connected to a computer running Ethovision (Leesburg, VA) software. Ethovision video tracking software measured the amount of time mice spent in each chamber and interacting with each mouse.

Home cage monitoring

Home cages were placed inside SmartFrame Cage Rack System (Hamilton/Kinder) frames connected to a computer running Hamilton/Kinder MotorMonitor software. Distance traveled was measured and averaged by the software by recording infrared photobeam breaks over a 24 h period.

Marble burying

Mice were habituated for 15 min in a standard 7″ × 11″ mouse cage containing 4 cm deep bedding. The mice were removed, 16 marbles evenly spaced atop the bedding, the mice were returned to the cage for 15 min, removed and the number of marbles buried was recorded.

Rotarod

The rotarod treadmill (Ugo Basile, Gemonio, Italy) consists of an automated rotating cylinder measuring 3 cm in diameter. Mice were given 10 trials (5 per day over 2 days, with a break of 20 min between each trial), where the treadmill accelerated from 0 to 32 rps. The speed at which each mouse fell was calculated using a stopwatch.

Open field

Mice were placed in a 50 cm (W) × 50 cm (L) × 50 cm (H) plexiglass arena for 10 min and total distanced travelled and time spent in the periphery versus center was measured using an overhead camera linked to a computer running Ethovision video software.

Light/dark box

Mice were tested in the two-chamber (dark and light) plexiglass apparatus and given a 10 min trial to move freely between the chambers. Time spent in each chamber was measured by infrared photobeam breaks using the Kinder Scientific© (Poway, CA) MotorMonitorII program in the MotorMonitorII light–dark frame configuration.

Immunoblotting

Immunoblotting of frontal cortex and hippocampal lysates were conducted as previously described (18). The following primary antibodies were used: β-catenin (Thermofisher, Waltham, MA, 1:2500 dilution), α-N-catenin (Cell Signaling, Danvers, MA, 1:1000), p120ctn (Abcam, Cambridge, MA, 1:500), N-cadherin (Cell Signaling, 1:1000), γ-catenin (BD Biosciences, San Jose, CA, 1:5000), S-SCAM (Sigma, Natick, MA, 1:250), plasma membrane Ca 2+ ATPase (PMCA) (Thermofisher, 1:10 000), LEF-1 (Cell Signaling, 1:1000), sp3 (Santa Cruz, Santa Cruz, CA, 1:100), glyceraldehyde 3-phosphate dehydrogenase (GAPDH), as loading control (Millipore, Burlington, MA, 1:50 000) and goat anti-mouse or goat anti-rat secondary antibodies conjugated to horseradish peroxidase (Jackson ImmunoResearch Laboratories, West Grove, PA).

Immunoprecipitation

Immunoprecipitation was performed with hippocampal and frontal cortex lysates with LEF-1 (Millipore) and γ-catenin (BD Biosciences) antibodies and Protein Agarose A/G PLUS beads (Santa Cruz) (18).

qPCR

Using the RNeasy Mini Kit (Qiagen), RNA extracted from β-cat cKO and control frontal cortex and hippocampus was used to generate cDNAs analyzed by quantitative PCR (qPCR) with the following primer sets (MGH Primer Bank): *ctnnb1*, *dkk1*, *c-myc*, *c-met*, *cycD1*, *lef-1*, *ctnnb1*, *ctnnd1*, *cdh2*, *ctnna2* and *gapdh* (endogenous control).

Spine density analysis

The β-cat cKO and control littermate mice were transcardially perfused with 4% paraformaldehyde, and the brains were processed for spine density analysis via gene gun delivery of microtungsten particles coated with the lipophilic fluorescent dye DiI (75) and super-resolution laser-scanning confocal microscopy (Zeiss, Oberkochen, Germany LSM800/880, Airyscan), conducted by a commercial service (Afraxis, San Diego, CA). Microscopy was performed blind to experimental conditions. Four mice per

genotype were analyzed and seven to eight neurons samples were analyzed. Spines were counted visually on the secondary apical dendrites of layer 3 mPFC pyramidal neurons and CA1 pyramidal neurons.

Statistics

All data were analyzed using GraphPad Prism 8 (GraphPad Software). Statistical analyses are indicated for each experiment in the Results section. All western blot and qPCR data are normalized to littermate control.

Supplementary Material

Supplementary Material is available at *HMG* online.

Acknowledgements

We thank members of the Jacob Lab for helpful discussions and insights.

Conflict of Interest statement. None declared.

Funding

National Institutes of Health (NIH) National Institute of Mental Health (1R01MH106623 to M.H.J.); National Institute of General Medical Sciences (K12GM074869 to R.J.W.); National Institute of Neurological Disorders and Stroke (P30 NS047243 to F.R.J.).

References

1. Ropers, H.H. (2010) Genetics of early onset cognitive impairment. *Annu. Rev. Genomics Hum. Genet.*, **11**, 161–187.
2. Flore, L.A. and Milunsky, J.M. (2012) Updates in the genetic evaluation of the child with global developmental delay or intellectual disability. *Semin. Pediatr. Neurol.*, **19**, 173–180.
3. La Malfa, G., Lassi, S., Bertelli, M., Salvini, R. and Placidi, G.F. (2004) Autism and intellectual disability: a study of prevalence on a sample of the Italian population. *J. Intellect. Disabil. Res.*, **48**, 262–267.
4. Tallantyre, E. and Robertson, N.P. (2013) Autism and intellectual disability. *J. Neurol.*, **260**, 936–939.
5. Hormozdiari, F., Penn, O., Borenstein, E. and Eichler, E.E. (2015) The discovery of integrated gene networks for autism and related disorders. *Genome Res.*, **25**, 142–154.
6. Krumm, N., O'Roak, B.J., Shendure, J. and Eichler, E.E. (2014) A de novo convergence of autism genetics and molecular neuroscience. *Trends Neurosci.*, **37**, 95–105.
7. Kuechler, A., Willemsen, M.H., Albrecht, B., Bacino, C.A., Bartholomew, D.W., van Bokhoven, H., van den Boogaard, M.J., Bramswig, N., Buttner, C., Cremer, K. *et al.* (2015) De novo mutations in beta-catenin (CTNNB1) appear to be a frequent cause of intellectual disability: expanding the mutational and clinical spectrum. *Hum. Genet.*, **134**, 97–109.
8. Dubruc, E., Putoux, A., Labalme, A., Rougeot, C., Sanlaville, D. and Edery, P. (2014) A new intellectual disability syndrome caused by CTNNB1 haploinsufficiency. *Am. J. Med. Genet. A*, **164A**, 1571–1575.
9. Kharbanda, M., Pilz, D.T., Tomkins, S., Chandler, K., Saggar, A., Fryer, A., McKay, V., Louro, P., Smith, J.C., Burn, J. *et al.* (2017) Clinical features associated with CTNNB1 de novo loss of function mutations in ten individuals. *Eur. J. Med. Genet.*, **60**, 130–135.
10. Winczewska-Wiktor, A., Badura-Stronka, M., Monies-Nowicka, A., Nowicki, M.M., Steinborn, B., Latos-Bielenska, A. and Monies, D. (2016) A de novo CTNNB1 nonsense mutation associated with syndromic atypical hyperekplexia, microcephaly and intellectual disability: a case report. *BMC Neurol.*, **16**, 35.
11. de Ligt, J., Willemsen, M.H., van Bon, B.W., Kleefstra, T., Yntema, H.G., Kroes, T., Vulto-van Silfhout, A.T., Koolen, D.A., de Vries, P., Gilissen, C. *et al.* (2012) Diagnostic exome sequencing in persons with severe intellectual disability. *N. Engl. J. Med.*, **367**, 1921–1929.
12. Yu, X. and Malenka, R.C. (2004) Multiple functions for the cadherin/catenin complex during neuronal development. *Neuropharmacology*, **47**, 779–786.
13. Brigidi, G.S. and Bamji, S.X. (2011) Cadherin–catenin adhesion complexes at the synapse. *Curr. Opin. Neurobiol.*, **21**, 208–214.
14. Uchida, N., Honjo, Y., Johnson, K.R., Wheelock, M.J. and Takeichi, M. (1996) The catenin/cadherin adhesion system is localized in synaptic junctions bordering transmitter release zones. *J. Cell Biol.*, **135**, 767–779.
15. Knudsen, K.A., Soler, A.P., Johnson, K.R. and Wheelock, M.J. (1995) Interaction of alpha-actinin with the cadherin/-catenin cell-cell adhesion complex via alpha-catenin. *J. Cell Biol.*, **130**, 67–77.
16. Nishimura, W., Yao, I., Iida, J., Tanaka, N. and Hata, Y. (2002) Interaction of synaptic scaffolding molecule and beta-catenin. *J. Neurosci.*, **22**, 757–765.
17. Mohn, J.L., Alexander, J., Pirone, A., Palka, C.D., Lee, S.Y., Mebane, L., Haydon, P.G. and Jacob, M.H. (2014) New molecular insights into cognitive and autistic-like disabilities. *Mol. Psychiatry*, **19**, 1053.
18. Mohn, J.L., Alexander, J., Pirone, A., Palka, C.D., Lee, S.Y., Mebane, L., Haydon, P.G. and Jacob, M.H. (2014) Adenomatous polyposis coli protein deletion leads to cognitive and autism-like disabilities. *Mol. Psychiatry*, **19**, 1133–1142.
19. Rosenberg, M.M., Yang, F., Mohn, J.L., Storer, E.K. and Jacob, M.H. (2010) The postsynaptic adenomatous polyposis coli (APC) multiprotein complex is required for localizing neuroligin and neurexin to neuronal nicotinic synapses in vivo. *J. Neurosci.*, **30**, 11073–11085.
20. Clevers, H. and Nusse, R. (2012) Wnt/beta-catenin signaling and disease. *Cell*, **149**, 1192–1205.
21. Kobayashi, M., Honma, T., Matsuda, Y., Suzuki, Y., Narisawa, R., Ajioka, Y. and Asakura, H. (2000) Nuclear translocation of beta-catenin in colorectal cancer. *Br. J. Cancer*, **82**, 1689–1693.
22. Simcha, I., Shtutman, M., Salomon, D., Zhurinsky, J., Sadot, E., Geiger, B. and Ben-Ze'ev, A. (1998) Differential nuclear translocation and transactivation potential of beta-catenin and plakoglobin. *J. Cell Biol.*, **141**, 1433–1448.
23. Park, M. and Shen, K. (2012) WNTs in synapse formation and neuronal circuitry. *EMBO J.*, **31**, 2697–2704.
24. Salinas, P.C. (2012) Wnt signaling in the vertebrate central nervous system: from axon guidance to synaptic function. *Cold Spring Harb. Perspect. Biol.*, **4**, 4:a008003.
25. Salinas, P.C. and Zou, Y. (2008) Wnt signaling in neural circuit assembly. *Annu. Rev. Neurosci.*, **31**, 339–358.
26. Rosso, S.B. and Inestrosa, N.C. (2013) WNT signaling in neuronal maturation and synaptogenesis. *Front. Cell. Neurosci.*, **7**, 103.
27. Takeichi, M., Uemura, T., Iwai, Y., Uchida, N., Inoue, T., Tanaka, T. and Suzuki, S.C. (1997) Cadherins in brain patterning and

neural network formation. *Cold Spring Harb. Symp. Quant. Biol.*, **62**, 505–510.
28. Uchida, N. and Takeichi, M. (1997) Role of cadherin adhesion systems in selective synapse formation. *Tanpakushitsu Kakusan Koso*, **42**, 525–534.
29. Mysore, S.P., Tai, C.Y. and Schuman, E.M. (2007) Effects of N-cadherin disruption on spine morphological dynamics. *Front. Cell. Neurosci.*, **1**, 1.
30. Seong, E., Yuan, L. and Arikkath, J. (2015) Cadherins and catenins in dendrite and synapse morphogenesis. *Cell Adh. Migr.*, **9**, 202–213.
31. Pirone, A., Alexander, J., Lau, L.A., Hampton, D., Zayachkivsky, A., Yee, A., Yee, A., Jacob, M.H. and Dulla, C.G. (2017) APC conditional knock-out mouse is a model of infantile spasms with elevated neuronal beta-catenin levels, neonatal spasms, and chronic seizures. *Neurobiol. Dis.*, **98**, 149–157.
32. Gould, T.D., O'Donnell, K.C., Picchini, A.M., Dow, E.R., Chen, G. and Manji, H.K. (2008) Generation and behavioral characterization of beta-catenin forebrain-specific conditional knockout mice. *Behav. Brain Res.*, **189**, 117–125.
33. Tucci, V., Kleefstra, T., Hardy, A., Heise, I., Maggi, S., Willemsen, M.H., Hilton, H., Esapa, C., Simon, M., Buenavista, M.T. *et al.* (2014) Dominant beta-catenin mutations cause intellectual disability with recognizable syndromic features. *J. Clin. Invest.*, **124**, 1468–1482.
34. Smith, A., Bourdeau, I., Wang, J. and Bondy, C.A. (2005) Expression of catenin family members CTNNA1, CTNNA2, CTNNB1 and JUP in the primate prefrontal cortex and hippocampus. *Brain Res. Mol. Brain Res.*, **135**, 225–231.
35. Brault, V., Moore, R., Kutsch, S., Ishibashi, M., Rowitch, D.H., McMahon, A.P., Sommer, L., Boussadia, O. and Kemler, R. (2001) Inactivation of the beta-catenin gene by Wnt1-Cre-mediated deletion results in dramatic brain malformation and failure of craniofacial development. *Development*, **128**, 1253–1264.
36. Rios, M., Fan, G., Fekete, C., Kelly, J., Bates, B., Kuehn, R., Lechan, R.M. and Jaenisch, R. (2001) Conditional deletion of brain-derived neurotrophic factor in the postnatal brain leads to obesity and hyperactivity. *Mol. Endocrinol.*, **15**, 1748–1757.
37. O'Roak, B.J., Vives, L., Girirajan, S., Karakoc, E., Krumm, N., Coe, B.P., Levy, R., Ko, A., Lee, C., Smith, J.D. *et al.* (2012) Sporadic autism exomes reveal a highly interconnected protein network of de novo mutations. *Nature*, **485**, 246–250.
38. Silverman, J.L., Yang, M., Lord, C., Crawley, J.N. (2010) Behavioural phenotyping assays for mouse models of autism. *Nat. Rev. Neurosci.*, **11**, 490–502.
39. Thomas, A., Burant, A., Bui, N., Graham, D., Yuva-Paylor, L.A. and Paylor, R. (2009) Marble burying reflects a repetitive and perseverative behavior more than novelty-induced anxiety. *Psychopharmacology (Berl.)*, **204**, 361–373.
40. Dias, C., Feng, J., Sun, H., Shao, N.Y., Mazei-Robison, M.S., Damez-Werno, D., Scobie, K., Bagot, R., LaBonte, B., Ribeiro, E. *et al.* (2014) Beta-catenin mediates stress resilience through Dicer1/microRNA regulation. *Nature*, **516**, 51–55.
41. Wisniewska, M.B. (2013) Physiological role of beta-catenin/TCF signaling in neurons of the adult brain. *Neurochem. Res.*, **38**, 1144–1155.
42. He, T.C., Sparks, A.B., Rago, C., Hermeking, H., Zawel, L., da Costa, L.T., Morin, P.J., Vogelstein, B. and Kinzler, K.W. (1998) Identification of c-MYC as a target of the APC pathway. *Science*, **281**, 1509–1512.
43. Filali, M., Cheng, N., Abbott, D., Leontiev, V. and Engelhardt, J.F. (2002) Wnt-3A/beta-catenin signaling induces transcription from the LEF-1 promoter. *J. Biol. Chem.*, **277**, 33398–33410.
44. Boon, E.M., van der Neut, R., van de Wetering, M., Clevers, H. and Pals, S.T. (2002) Wnt signaling regulates expression of the receptor tyrosine kinase met in colorectal cancer. *Cancer Res.*, **62**, 5126–5128.
45. Zhurinsky, J., Shtutman, M. and Ben-Ze'ev, A. (2000) Plakoglobin and beta-catenin: protein interactions, regulation and biological roles. *J. Cell Sci.*, **113**, 3127–3139.
46. Elia, L.P., Yamamoto, M., Zang, K. and Reichardt, L.F. (2006) p120 catenin regulates dendritic spine and synapse development through rho-family GTPases and cadherins. *Neuron*, **51**, 43–56.
47. Yuan, L. and Arikkath, J. (2017) Functional roles of p120ctn family of proteins in central neurons. *Semin. Cell Dev. Biol.*, **69**, 70–82.
48. Yuan, L., Seong, E., Beuscher, J.L. and Arikkath, J. (2015) Delta-catenin regulates spine architecture via cadherin and PDZ-dependent interactions. *J. Biol. Chem.*, **290**, 10947–10957.
49. Lee, S.H., Peng, I.F., Ng, Y.G., Yanagisawa, M., Bamji, S.X., Elia, L.P., Balsamo, J., Lilien, J., Anastasiadis, P.Z., Ullian, E.M. *et al.* (2008) Synapses are regulated by the cytoplasmic tyrosine kinase Fer in a pathway mediated by p120catenin, Fer, SHP-2, and beta-catenin. *J. Cell Biol.*, **183**, 893–908.
50. Deng, F., Price, M.G., Davis, C.F., Mori, M. and Burgess, D.L. (2006) Stargazin and other transmembrane AMPA receptor regulating proteins interact with synaptic scaffolding protein MAGI-2 in brain. *J. Neurosci.*, **26**, 7875–7884.
51. Yu, X. and Malenka, R.C. (2003) Beta-catenin is critical for dendritic morphogenesis. *Nat. Neurosci.*, **6**, 1169–1177.
52. Arikkath, J. and Reichardt, L.F. (2008) Cadherins and catenins at synapses: roles in synaptogenesis and synaptic plasticity. *Trends Neurosci.*, **31**, 487–494.
53. Friedman, L.G., Benson, D.L. and Huntley, G.W. (2015) Cadherin-based transsynaptic networks in establishing and modifying neural connectivity. *Curr. Top. Dev. Biol.*, **112**, 415–465.
54. Wolff, J.J. and Symons, F.J. (2013) An evaluation of multicomponent exposure treatment of needle phobia in an adult with autism and intellectual disability. *J. Appl. Res. Intellect. Disabil.*, **26**, 344–348.
55. O'Roak, B.J., Deriziotis, P., Lee, C., Vives, L., Schwartz, J.J., Girirajan, S., Karakoc, E., Mackenzie, A.P., Ng, S.B., Baker, C. *et al.* (2011) Exome sequencing in sporadic autism spectrum disorders identifies severe de novo mutations. *Nat. Genet.*, **43**, 585–589.
56. Fossat, N., Jones, V., Khoo, P.L., Bogani, D., Hardy, A., Steiner, K., Mukhopadhyay, M., Westphal, H., Nolan, P.M., Arkell, R. *et al.* (2011) Stringent requirement of a proper level of canonical WNT signalling activity for head formation in mouse embryo. *Development*, **138**, 667–676.
57. Nikitczuk, J.S., Patil, S.B., Matikainen-Ankney, B.A., Scarpa, J., Shapiro, M.L., Benson, D.L. and Huntley, G.W. (2014) N-cadherin regulates molecular organization of excitatory and inhibitory synaptic circuits in adult hippocampus in vivo. *Hippocampus*, **24**, 943–962.
58. Park, C., Falls, W., Finger, J.H., Longo-Guess, C.M. and Ackerman, S.L. (2002) Deletion in Catna2, encoding alpha N-catenin, causes cerebellar and hippocampal lamination defects and impaired startle modulation. *Nat. Genet.*, **31**, 279–284.
59. Maguschak, K.A. and Ressler, K.J. (2008) Beta-catenin is required for memory consolidation. *Nat. Neurosci.*, **11**, 1319–1326.

60. Dong, F., Jiang, J., McSweeney, C., Zou, D., Liu, L. and Mao, Y. (2016) Deletion of CTNNB1 in inhibitory circuitry contributes to autism-associated behavioral defects. *Hum. Mol. Genet.*, **25**, 2738–2751.
61. Akins, M.R. and Greer, C.A. (2006) Axon behavior in the olfactory nerve reflects the involvement of catenin-cadherin mediated adhesion. *J. Comp. Neurol.*, **499**, 979–989.
62. Maeda, O., Usami, N., Kondo, M., Takahashi, M., Goto, H., Shimokata, K., Kusugami, K. and Sekido, Y. (2004) Plakoglobin (gamma-catenin) has TCF/LEF family-dependent transcriptional activity in beta-catenin-deficient cell line. *Oncogene*, **23**, 964–972.
63. Solanas, G., Miravet, S., Casagolda, D., Castano, J., Raurell, I., Corrionero, A., Garcia de Herreros, A. and Dunach, M. (2016) Beta-catenin and plakoglobin N- and C-tails determine ligand specificity. *J. Biol. Chem.*, **291**, 23925–23927.
64. Solanas, G., Miravet, S., Casagolda, D., Castano, J., Raurell, I., Corrionero, A., de Herreros, A.G. and Dunach, M. (2004) Beta-catenin and plakoglobin N- and C-tails determine ligand specificity. *J. Biol. Chem.*, **279**, 49849–49856.
65. Huber, A.H. and Weis, W.I. (2001) The structure of the beta-catenin/E-cadherin complex and the molecular basis of diverse ligand recognition by beta-catenin. *Cell*, **105**, 391–402.
66. Huber, A.H., Stewart, D.B., Laurents, D.V., Nelson, W.J. and Weis, W.I. (2001) The cadherin cytoplasmic domain is unstructured in the absence of beta-catenin. A possible mechanism for regulating cadherin turnover. *J. Biol. Chem.*, **276**, 12301–12309.
67. Maruo, T., Sakakibara, S., Miyata, M., Itoh, Y., Kurita, S., Mandai, K., Sasaki, T. and Takai, Y. (2018) Involvement of l-afadin, but not s-afadin, in the formation of puncta adherentia junctions of hippocampal synapses. *Mol. Cell. Neurosci.*, **92**, 40–49.
68. Birukova, A.A., Fu, P., Wu, T., Dubrovskyi, O., Sarich, N., Poroyko, V. and Birukov, K.G. (2012) Afadin controls p120-catenin-ZO-1 interactions leading to endothelial barrier enhancement by oxidized phospholipids. *J. Cell. Physiol.*, **227**, 1883–1890.
69. Sato, T., Fujita, N., Yamada, A., Ooshio, T., Okamoto, R., Irie, K. and Takai, Y. (2006) Regulation of the assembly and adhesion activity of E-cadherin by nectin and afadin for the formation of adherens junctions in Madin–Darby canine kidney cells. *J. Biol. Chem.*, **281**, 5288–5299.
70. Majima, T., Ogita, H., Yamada, T., Amano, H., Togashi, H., Sakisaka, T., Tanaka-Okamoto, M., Ishizaki, H., Miyoshi, J. and Takai, Y. (2009) Involvement of afadin in the formation and remodeling of synapses in the hippocampus. *Biochem. Biophys. Res. Commun.*, **385**, 539–544.
71. Perego, C., Vanoni, C., Massari, S., Longhi, R. and Pietrini, G. (2000) Mammalian LIN-7 PDZ proteins associate with beta-catenin at the cell-cell junctions of epithelia and neurons. *EMBO J.*, **19**, 3978–3989.
72. Zhu, W., Li, J., Chen, S., Zhang, J., Vetrini, F., Braxton, A., Eng, C.M., Yang, Y., Xia, F., Keller, K.L. *et al.* (2018) Two de novo novel mutations in one SHANK3 allele in a patient with autism and moderate intellectual disability. *Am. J. Med. Genet. A*, **176**, 973–979.
73. Gujral, T.S., Karp, E.S., Chan, M., Chang, B.H. and MacBeath, G. (2013) Family-wide investigation of PDZ domain-mediated protein–protein interactions implicates beta-catenin in maintaining the integrity of tight junctions. *Chem. Biol.*, **20**, 816–827.
74. Moy, S.S., Nadler, J.J., Young, N.B., Perez, A., Holloway, L.P., Barbaro, R.P., Barbaro, J.R., Wilson, L.M., Threadgill, D.W., Lauder, J.M. *et al.* (2007) Mouse behavioral tasks relevant to autism: phenotypes of 10 inbred strains. *Behav. Brain Res.*, **176**, 4–20.
75. Gan, W.B., Grutzendler, J., Wong, W.T., Wong, R.O. and Lichtman, J.W. (2000) Multicolor "DiOlistic" labeling of the nervous system using lipophilic dye combinations. *Neuron*, **27**, 219–225.